REVIEWS

Journal of Semiconductors
(2019) 40, 081510
doi: 10.1088/1674-4926/40/8/081510

Amorphous magnetic semiconductors with Curie temperatures above room temperature

Na Chen[1, †], Kaixuan Fang[1], Hongxia Zhang[1], Yingqi Zhang[1], Wenjian Liu[1], Kefu Yao[1], and Zhengjun Zhang[2]

[1]Key Laboratory for Advanced Materials Processing Technology (MOE), School of Materials Science and Engineering, Tsinghua University, Beijing 100084, China

[2]Key Laboratory for Advanced Materials (MOE), School of Materials Science and Engineering, Tsinghua University, Beijing 100084, China

Abstract: Recently, amorphous magnetic semiconductors as a new family of magnetic semiconductors have been developed by oxidizing ferromagnetic amorphous metals/alloys. Intriguingly, tuning the relative atomic ratios of Co and Fe in a Co-Fe-Ta-B-O system leads to the formation of an intrinsic magnetic semiconductor. Starting from high Curie-temperature amorphous ferromagnets, these amorphous magnetic semiconductors show Curie temperatures well above room temperature. Among them, one typical example is a p-type $Co_{28.6}Fe_{12.4}Ta_{4.3}B_{8.7}O_{46}$ magnetic semiconductor, which has an optical bandgap of ~2.4 eV, room-temperature saturation magnetization of ~433 emu/cm^3, and the Curie temperature above 600 K. The amorphous $Co_{28.6}Fe_{12.4}Ta_{4.3}B_{8.7}O_{46}$ magnetic semiconductor can be integrated with n-type Si to form p–n heterojunctions with a threshold voltage of ~1.6 V, validating its p-type semiconducting character. Furthermore, the demonstration of electric field control of its room-temperature ferromagnetism reflects the interplay between the electricity and ferromagnetism in this material. It is suggested that the carrier density, ferromagnetism and conduction type of an intrinsic magnetic semiconductor are controllable by means of an electric field effect. These findings may pave a new way to realize magnetic semiconductor-based spintronic devices that work at room temperature.

Key words: CoFeTaBO; amorphous magnetic semiconductors; electric field control of ferromagnetism; metal–semiconductor transition

Citation: N Chen, K X Fang, H X Zhang, Y Q Zhang, W J Liu, K F Yao, and Z J Zhang, Amorphous magnetic semiconductors with Curie temperatures above room temperature[J]. *J. Semicond.*, 2019, 40(8), 081510. http://doi.org/10.1088/1674-4926/40/8/081510

1. Introduction

The core functions of current-generation computers are to process, communicate and store information. These operations are mainly realized by two fundamental components of microprocessors and hard disks in computers, respectively. Si-based semiconductors are the key materials in microprocessors to enable the control of charges for transmitting and processing data, while ferromagnets provide the spin of electrons to be utilized for storing data on the hard disk. Generally, semiconductivity and ferromagnetism do not coexist in a material. However, it was found that europium chalcogenides showed anomalous optical, magnetic and transport phenomena[1, 2]. The physics behind this anomaly results from the strong *d*–*f* exchange interaction between the magnetic-exciton electrons of 5*d* band and the conduction 4*f* electrons[2]. As a result, there exists a relationship between the Curie temperature and the conduction electron concentration of these semiconducting europium chalcogenides. Based on these phenomena, Methfessel first proposed the concept of ferromagnetic semiconductor, whose magnetic properties could be modified by carrier injection, electrostatic fields or other means that changed the free carrier concentration in semiconductors[3]; that is, both the charge and spin of electrons can be manipulated simultaneously in these ferromagnetic semiconductors. The europium chalcogenides are therefore regarded as the first generation ferromagnetic semiconductors. Despite their scientific importance, these magnetic rare earth compounds usually have complex crystalline structures, which are different from those of the widely used semiconductor materials such as Si and GaAs. It is difficult to obtain high-quality interface structure when integrating them with Si or GaAs. In addition, most of them show Curie temperatures far below room temperature[3].

To maintain the most attractive semiconducting properties used in electronic devices, an approach was proposed to introduce magnetic elements into non-magnetic semiconductors for creating new type of magnetic semiconductors (MSs) called diluted magnetic semiconductors (DMSs)[4–6]. With the ever growing necessity of miniaturization of future electronic devices, DMSs have stimulated intense interest due to their potential for realizing new functionalities and revolutionizing device concepts. The most thoroughly investigated DMSs are (Ga, Mn)As and (In, Mn)As systems based on III–V semiconductors[7, 8]. Chen *et al.* explored nanostructure engineering to enhance the Curie temperature of the (Ga, Mn)As DMS up to 200 K, which has been the highest value recorded for this system[9]. Further increasing the Curie temperatures of DMSs above room temperature is a challenging task[10–20]. The basic reason for this is the limitation of the solid solubility for magnetic elements to dissolve in these DMSs. To keep the original lattice structure of the host crystal, the solubility of magnetic elements is very low especially for those with the electronegativ-

Correspondence to: N Chen, chennadm@mail.tsinghua.edu.cn
Received 3 JUNE 2019; Revised 14 JUNE 2019.

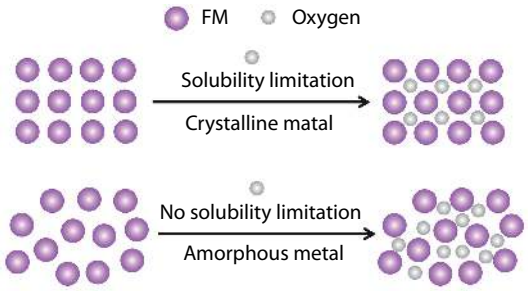

Fig. 1. (Color online) Schematic diagram for including oxygen in crystalline and amorphous metals. FM denotes ferromagnetic metals.

ity and valence electron concentrations significantly different from the base elements[21–23]. This becomes the key barrier to creating high Curie-temperature DMSs that work at room temperature.

In contrast to the approach for developing the DMSs, we found a different way to create a new kind of MSs. First, we selected a high Curie-temperature ferromagnetic amorphous alloy (AA) as a host. Second, we introduced oxygen into this AA in a well-controlled manner. AAs are mainly characterized by non-directional and non-saturated metallic bonds. Their disordered atomic structures and unique electronic structures enable them to be nice hosts to include a large quantity of foreign elements[24–26]. Oxidizing the ferromagnetic AA leads to a metal–semiconductor transtion and causes the formation of amorphous MSs (AMSs) with Curie temperatures well above room temperature[26].

2. Amorphous magnetic semiconductors

2.1. Metal–semiconductor transition in amorphous alloys

Crystalline metals and AAs behave quite differently as oxygen is introduced into them, respectively (Fig. 1). The solubility of oxygen in a crystalline metal limits the maximal amount of oxygen that enters its lattice structure, whereas no similar limitation exists for oxygen to be included in an AA. Moreover, amorphous materials could access to lower energy states through structural relaxation[27–31]. Local atomic rearrangement reduces local strains induced by the oxygen addition, thereby permiting more oxygen atoms to be included in amorphous materials. With increasing the oxygen content, the conduction electrons of the AA are gradually localized due to the formation of ionic or/and covalent bonds between the constituents of the AA and the included oxygen atoms. One can expect that the original AA becomes more and more insulating as the oxygen content continuously increases. As a result, a metal–semiconductor transition occurs at a critical value of the oxygen content.

Following the idea of transferring AAs to semiconductors, an alloy system is selected owing to the following three reasons. First, ferromagnetic alloys are preferred in order to obtain MSs with a combination of desirable functionalities. Moreover, the Curie temperatures of the selected alloy systems should be higher than 500 K, which is required for a ferromagnet to work in practical applications[32]. For amorphous ferromagnets, it is thus better to select AA systems containing 3*d* transition metal elements of Fe and/or Co, contributing to their robust ferromagnetism. Second, the ferromagnetism of the selected AA should be sustained even after it is heavily oxidized. To achieve this, the ferromagnetic metals in the alloy system are better to have smaller affinity for oxygen than the other constituents. Hence, the ferromagnetic metal elements are least oxidized compared with other constitutes in the alloy system. Third, the selected AA system should be a good glass former so that it can maintain its amorphous structure even when a high oxygen content is added. Based on these considerations, a good glass former Co–Fe–Ta–B system was selected[33, 34].

The Co–Fe–Ta–B–O thin films were deposited by radio frequency (RF) magnetron sputtering with an alloy target under a gas mixture of argon and oxygen[24–26]. Varying the oxygen partial pressure led to the formation of amorphous Co–Fe–Ta–B–O thin films with different oxygen contents. Ta and B were firstly oxidized and diffused out to form the surface oxide. The surface metal oxide increased with increasing the oxygen content. They contacted with each other by forming a continuous network (Fig. 2). The size of the inner AA nanoparticles became smaller and smaller. At a critical oxygen content, the AA phase disappeared and a single oxide phase was formed.

The structure of the $(Co_{0.53}Fe_{0.23}Ta_{0.08}B_{0.16})_{100-x}O_x$ ($0 \leqslant x \leqslant 50$ at%, abbreviated as $CFTBO_x$ hereafter) samples evolved gradually with increasing the oxygen content. High resolution transmission electron microscopy (HRTEM) images and selected area electron diffraction (SAED) patterns were taken for the $CFTBO_x$ system, respectively (Fig. 3). The $Co_{53}Fe_{23}Ta_8B_{16}$ AA shows maze-like atomic arrangements typical for amorphous structure (Fig. 3(a)). Its SAED pattern further verifies the formation of a single amorphous phase in the AA (Fig. 3(b)). With increasing the oxygen content above 15 at.%, an amorphous oxide (AO) phase emerges in the $CFTBO_x$ thin films. Fig. 3(c) shows the formation of a dual phase nanocomposite in the $CFTBO_{44}$ thin film, comprising the nanometer-sized AA particles embedded in the AO matrix. Its SAED pattern exhibits two sets of halos (Fig. 3(d)). One arises from the AA nanoparticles (Figs. 3(b) and 3(d)), while the other originates from the AO matrix (Figs. 3(d) and 3(f)). Further increasing the oxygen content to 46 at.% enables the formation of a single AO phase (Fig. 3(e)). The SAED pattern only shows the broad diffraction halo resulting from the single AO phase, which is semiconducting and ferromagnetic[26].

2.2. Optical, electrical and magnetic properties

Fig. 4(a) shows optical transmittance of the $CFTBO_x$ samples at thickness of ~100 nm. With increasing the oxygen content, their optical transmittance increases as well. The optical bandgap of the $CFTBO_{46}$ thin film is estimated to be about 2.4 eV based on the Tauc plot (Fig. 4(b)). In addition, the thin film exhibits 488 nm-peaked photoluminescence specturm, correpsonding to a photon energy of about 2.5 eV for blue light. This value is in consistent with its optical bandgap energy.

As the charge carrier concentration decreases with the oxygen content, the bandgap of the $CFTBO_x$ samples is gradually opened. That is, metal-semiconductor-insulator transitions are induced through this simple oxidization of the ferromagnetic AA. As a result, the resistivity of the $CFTBO_x$ samples increases with increasing the oxygen content (Fig. 5). The $CFTBO_{46}$ thin film exhibits a negative temperature dependence of $\ln(\rho/\rho_0)$–$1/T^{1/2}$ (inset of Fig. 5), characteristic of a semiconduct-

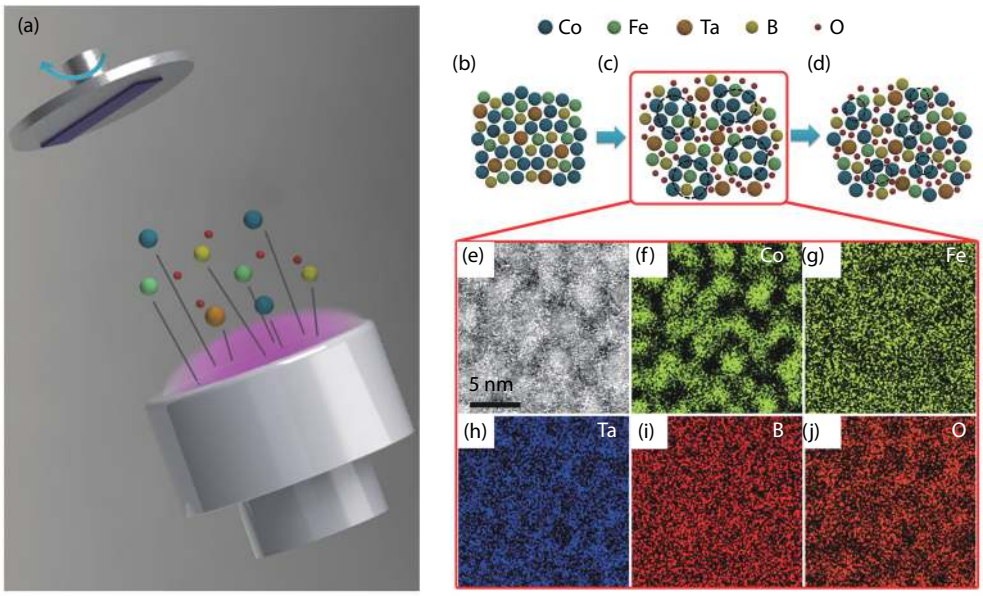

Fig. 2. (Color online) (a) Schematic diagram for depositing Co–Fe–Ta–B–O thin films. (b)–(j) oxidation process.

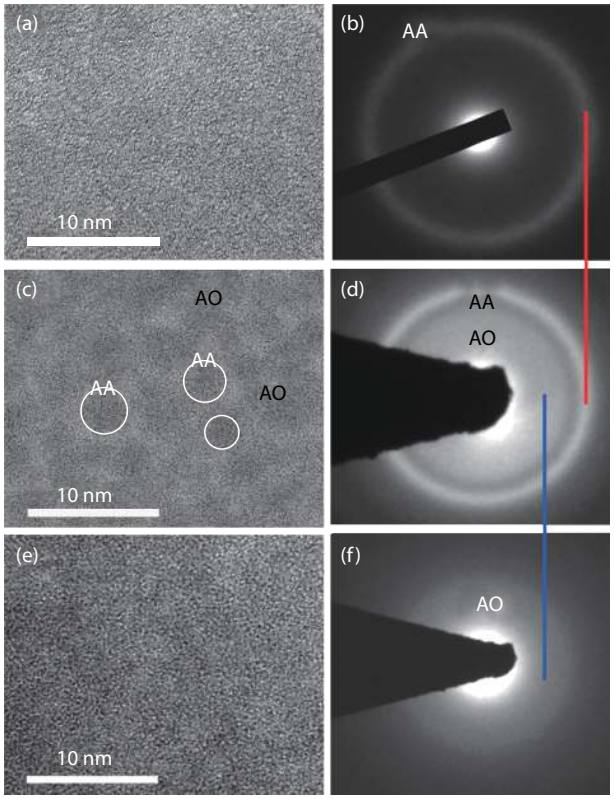

Fig. 3. (Color online) High-resolution transmission electron microscopy (HRTEM) images of the $CFTBO_x$ system (a) CFTB, (b) $CFTBO_{44}$, and (c) $CFTBO_{46}$.

or behavior. Further increasing the oxygen content above 60 at.% makes the $CFTBO_x$ samples become insulating.

The magnetic properties of the $CFTBO_x$ thin films are shown in Fig. 6. All the thin films are ferromagnetic at the oxygen contents ranging from 16 to 46 at.%. Noted that the saturation magnetization (M_s) of these thin films measured at room temperature increases from 728 to 867 emu/cm^3 as the oxygen content increases from 16 to 25 at.%. With further increasing in the oxygen content up to 46 at.%, M_s decreases from 867 to 433 emu/cm^3 (Figs. 6(a) and 6(b)). Furthermore, the zero-field cooling (ZFC) curve of the thin film with a low oxygen content of 16 at.% coincides with its field cooling (FC) curve, which is similar to that of the Co–Fe–Ta–B AA without containing oxygen[35, 36]. However, the ZFC curves of the $CFTBO_x$ thin films with the oxygen contents above 16 at.% deviate from their FC curves at low temperatures, demonstrating spin-glass-like maximum below 100 K. It is suggested that the spin-glass-like behavior is associated with the formation of the magnetic AO phase.

The high-temperature magnetization–temperature (M–T) curve of the $CFTBO_{46}$ sample shows that its glass transition occurs at about 600 K. The thin film is still ferromagnetic before the glass transition sets in. Therefore, the thin film should have a Curiecurie temperature above 600 K. At about 700 K, the magnetization increases owing to the apparent crystallization, similar to that found in $Co_{16}Fe_{68}Hf_9B_7$ alloy[37, 38]. Together with its electrical behavior, it can be concluded that the $CFTBO_{46}$ thin film is semiconducting and ferromagnetic. A new type of AMSs has been developed with a high Curie temperature above 600 K through simply oxidizing an originally ferromagnetic alloy . The conduction type of this AMS is determined to be p-type[26].

3. Prototype devices based on the amorphous magnetic semiconductors

3.1. Fabrication of p–n heterojunctions

Based on the above results, it is suggested that the single-phase $CFTBO_{46}$ thin film is an AMS with a Curie temperature above 600 K. Integrated with a heavily doped n-type Si, p–n and p–n–p heterojunctions were fabricated (Figs. 7(a) and 7(b)). Their current–voltage (I–V) curves are shown in Fig. 7(c). The threshold voltage (V_{th}) is about 1.6 eV for the p–n heterojunction, whereas no current flows in the p–n–p heterojunctions.

The voltage difference (V_D) built inside the p–n heterojunction can be described by the following equation:

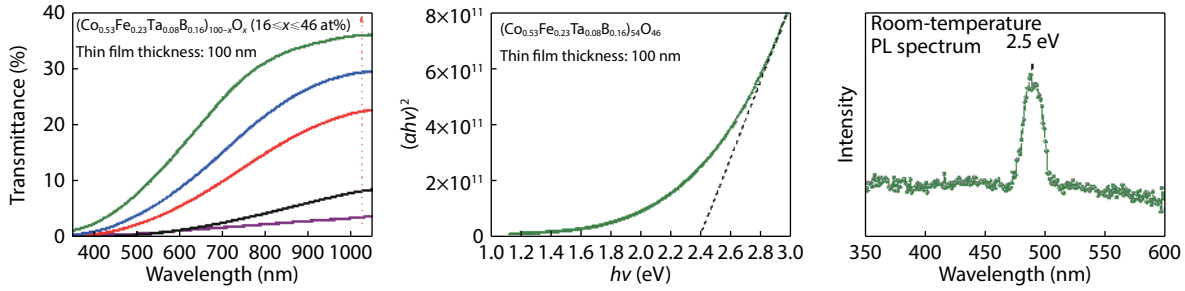

Fig. 4. (Color online) (a) Optical transmittance of the $CFTBO_x$ system. (b) Optical bandgap and (c) photoluminescence spectrum of the $CFTBO_{46}$ thin film.

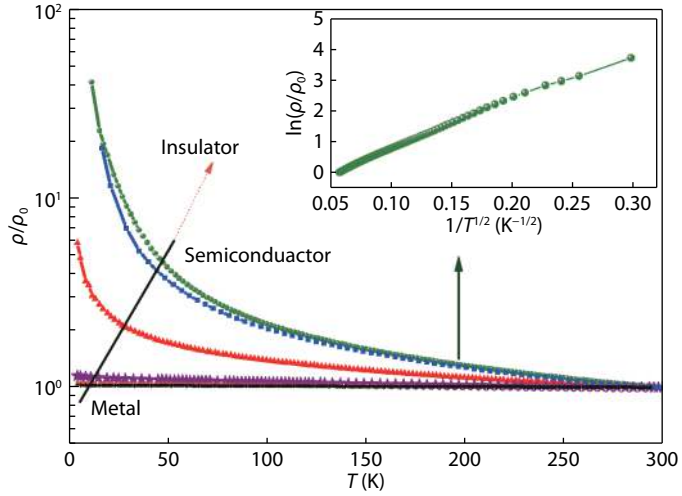

Fig. 5. (Color online) The normalized resistivity ρ/ρ_0 as a function of temperature (ρ_0 is the room temperature resistivity) for the $CFTBO_x$ ($16 \leqslant x \leqslant 46$ at%) thin films. Inset is the plot of $\ln(\rho/\rho_0)$ versus $1/T^{1/2}$ based on the experimental data of the $CFTBO_{46}$ thin film.

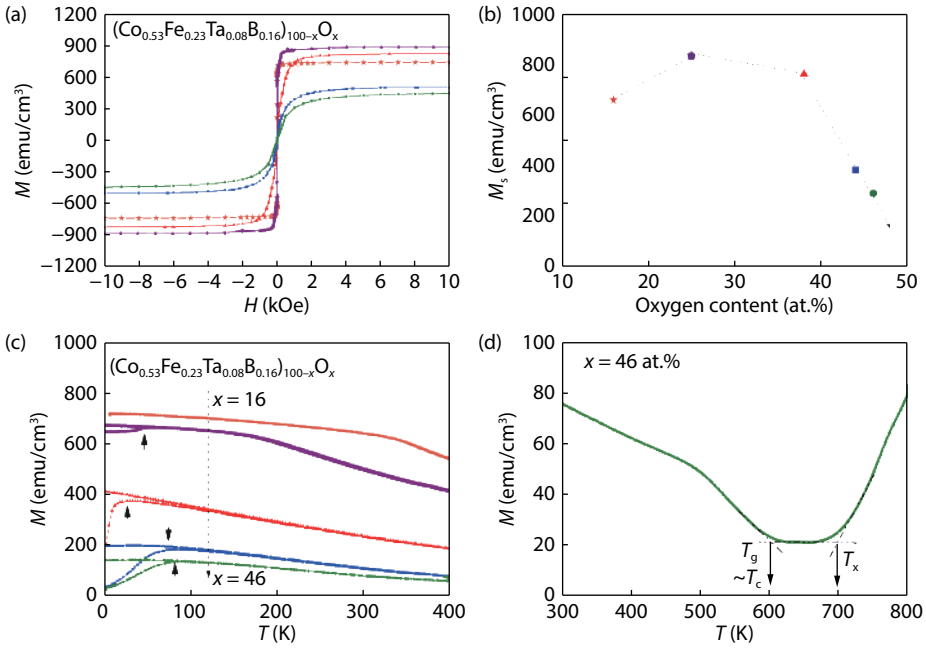

Fig. 6. (Color online) Magnetic behavior of the $CFTBO_x$ ($16 \leqslant x \leqslant 46$ at%): (a) Magnetic field dependence of the magnetization (M–H) curves measured at room temperature. (b) Saturation magnetization (M_s) variation with the oxygen contents. (c) Zero-field-cooling (ZFC) and field-cooling (FC) curves measured at an external field of 100 Oe. (d) High-temperature magnetization–temperature (M–T) curve measured for the $CFTBO_{46}$ thin film at an external field of 100 Oe.

$$V_{\mathrm{D}} = \frac{1}{q}\left(E_{\mathrm{i}2} - E_{\mathrm{i}1} + kT\ln\frac{N_{\mathrm{A}}N_{\mathrm{D}}}{n_{\mathrm{i}1}n_{\mathrm{i}2}}\right). \quad (1)$$

In the equation, q denotes the electron charge, $E_{\mathrm{i}2}$ and $E_{\mathrm{i}1}$ denote the Fermi energy levels of the intrinsic states of Si and

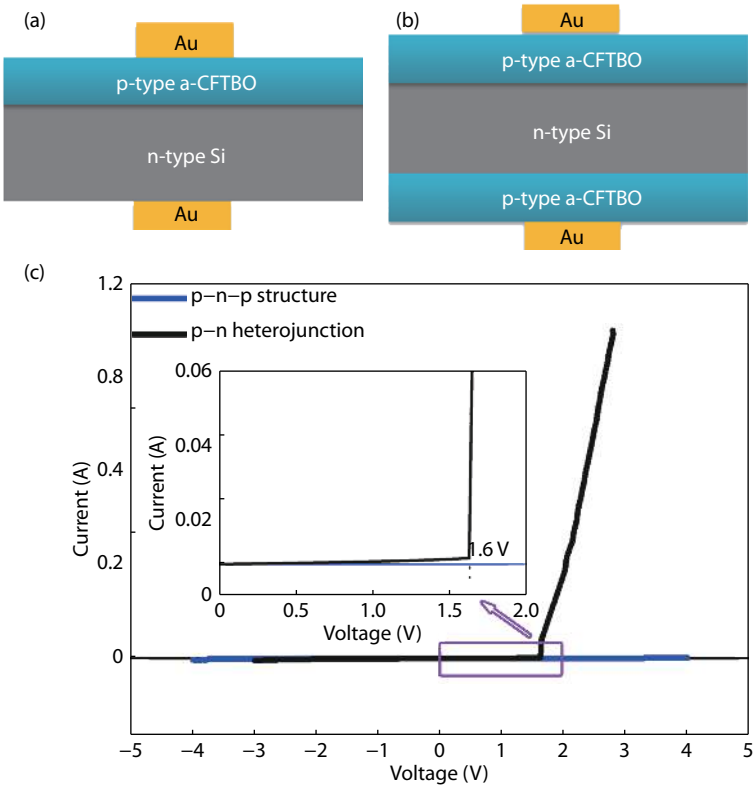

Fig. 7. (Color online) Schematic diagrams for fabricating p–n (b) and p–n–p heterojunctions based on the $CFTBO_{46}$ thin film and n-type Si. The Si is heavily doped with phosphorous and has resistivity of order of 10^{-3} Ω·cm. (c) The *I*–*V* curves for the heterojunctions of (a) and (b). The figure was adopted from Ref. [26].

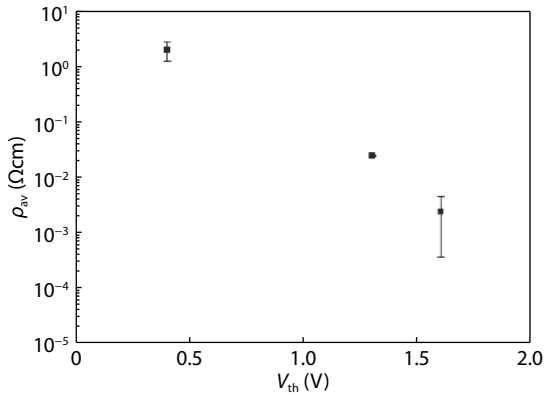

Fig. 8. The threshold voltage (V_{th}) of the p–n heterojunctions increasing with decreasing the resistivity (ρ) of the n-type Si.

$CFTBO_x$ thin films, respectively, k denotes the Boltzmann constant, T denotes the temperature, N_A and N_D denote the carrier concentrations of the $CFTBO_{46}$ thin film and n-type Si, respectively, n_{i1} and n_{i2} denote the intrinsic carrier concentrations of the $CFTBO_x$ and Si, respectively. Assuming that E_{i2}, E_{i1}, N_A, n_{i1} and n_{i2} are constants, V_D increases with N_D. A higher N_D indicates a lower ρ for n-type Si. Meanwhile, V_{th} of the p–n heterojunction is required to be larger than V_D for the forward conduction current to flow. As a consequence, V_{th} decreases with increasing ρ of the n-type Si as shown in Fig. 8.

3.2. Electric-field control of the ferromagnetism

Magnetic properties of ferromagnets are thought to be their inherent characteristics of the response to external magnetic fields. These magnetic properties are difficult to be changed once they are prepared[39]. However, the electrical control provides an alternative route to effectively manipulate the spin degree of freedom in ferromagnets. The first experimental observation of the electric-field control of the ferromagnetism was reported in the (In, Mn)As DMS[40], triggering intensive research interest in this subject. Hitherto, the electric-field control of the ferromagnetism has been realized in a variety of magnetic materials including metals, semiconductors and oxides[41–43], which may allow the development of low-power and non-volatile spintronic devices[44]. The physics behind the electric-field control of ferromagnetism results from the interplay between the carrier spins and local magnetic moments, which can be correlated with the carrier densities of various magnetic materials.

Fig. 9(a) shows a schematic diagram of a field effecttransistor (FET) with HfO_2 (2 nm)/ $CFTBO_{46}$ (25 nm)/Au/Cr/Si heterostructure. Through an ionic liquid (DEME-TFSI) dropped on the surface of the $CFTBO_{46}$ thin film, the gate voltage (V_G) is applied by forming an electric double layer (EDL) to achieve a large variation in its carrier density. Such a method has proven to be effective for realizing the stable modulation of carrier densities even when the gate voltage is removed[45–48]. In addition, the EDL transistor technique has been used for the electric-field control of ferromagnetism in several ferromagnets[49–51], which works beyond the fundamental limitation of the charge screening effect[52]. By varying V_G from –1.2 to 1.2 V, the room-temperature magnetization of the $CFTBO_{46}$ thin film is significantly altered by the applied electric field (Fig. 9(b)). When V_G is negative, the electrons of the $CFTBO_{46}$ thin film move down along the opposite direction of the applied electric field. As a result, its M_s increases. This indicates that its

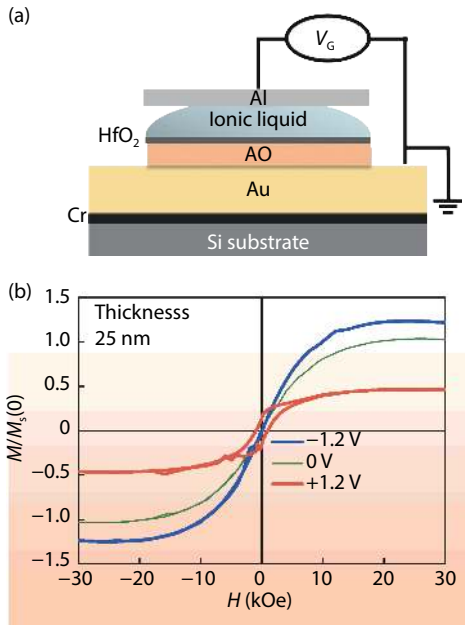

Fig. 9. (Color online) Electric-field control of the ferromagnetism in the $CFTBO_{46}$ AMS. (a) Schematic diagram of the experimental set-up for applying gate voltages (V_G) on the thin films through a drop of ionic liquid. The thickness of an insulating HfO_2 layer is about 2 nm. (b) Variation of M–H curves with different V_G measured at 300 K.

carrier concentration increases. Correspondingly, a positive V_G leads to a decrease in its hole concentration. Its M_s decreases. These experimental results indicate that the magnetic behavior of the $CFTBO_{46}$ MS can be modulated by electrical means. The presence of exchange interaction between the holes and localized magnetic moments in the thin film affects its ferromagnetism.

3.3. Development of an intrinsic magnetic semiconductor

The present $CFTBO_{46}$ MS is a p-type semiconductor. It is found that most of the existing AOs are n-type and are notoriously doped in p-type. Moreover, the control of their electrical conduction type remains a challenge. The conduction type of the AOs is determined by their local atomic configuration and the valence states of the involved metal cations[53].

To alter the conduction type of the present Co–Fe–Ta–B–O system, we modified the relative atomic ratios of Co and Fe in the system. As shown in Fig. 10(a), a new single-phase AO is developed. Its HRTEM image presents a maze-like pattern characterizing single-phase amorphous structure formed in the Co–Fe–Ta–B–O thin film. The electric-field control of its ferromagnetism is different from that of the p-type $CFTBO_{46}$ MS. No matter whether V_G is positive or negative, its M_s increases. It is suggested that the newly developed Co–Fe–Ta–B-O sample could be an intrinsic MS. Based on this intrinsic MS, we may use V_G to control its electrical conduction

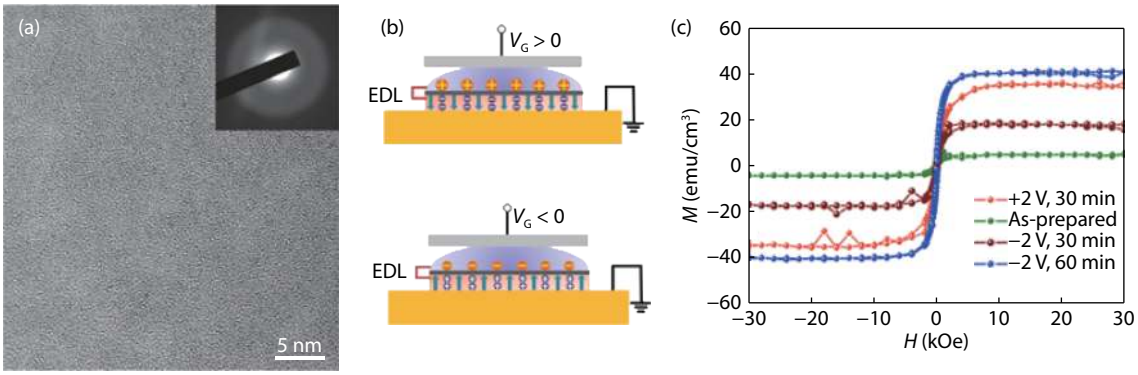

Fig. 10. (Color online) (a) HRTEM image of the newly developed CFTBO AMS. (b) Schematic diagrams for the electric-field control of carrier concentrations at different V_G. (c) M_s increaisng with both positive and negative V_G.

type of the different parts within the material, which would form a p–n junction at the interface between the different parts. To the best of our knowledge, this should be the first demonstration of an intrinsic MS. Meanwhile, the conduction type of this intrinsic MS can be tuned to be n-type or p-type by using an external electric field.

4. Conclusions and future perspectives

A new type of AMSs was developed by oxidizing originally ferromagnetic AAs. These AMSs showed high Curie temperatures well above room temperature. Based on them, prototype p–n heterojunctions were fabricated. Owing to the interplay between the holes and local magnetic moments, the electric-field control of ferromagnetism was realized at room temperature in these AMSs. The realization of high-Curie-temperature AMSs offers an opportunity to create next generation spintronic devices such as spin-diodes and spin-field effect transistors. The carrier mobility of amorphous materials is known to be very low. Therefore, these AMSs could not be good channel materials to be used in semiconductor-based devices. However, new phenomena may emerge at the interface between two AMSs if they are integrated together to form a field effect transistor. Therefore, furthering our understanding of the possible unprecedented interface effects may help to design and develop high performance spintronic devices based on these AMSs.

Future research subjects related to this new type of AMSs will be focused on the following three aspects:

(1) Both p-type and n-type AMSs are important for fabricating magnetic p-n diodes or spintronic transistors. The control of electrical conduction type in these AMSs should be possible through the compositional tuning based on the Co–Fe–Ta–B–O system. In this way, n-type AMSs could be developed to show high Curie temperature well above room temperature.

(2) New kinds of high performance MSs could be de-

veloped based on various ferromagnetic AAs. For example, the Co–Fe–Nb–B system is similar to the Co–Fe–Ta–B system. Oxidizing the Co–Fe–Nb–B AAs may lead to the formation of new AMSs with different properties. In addition to oxygen, nitrogen or sulfur can be used as elemental additions to transfer a ferromagnetic AA to AMSs. On the other hand, the precise characterization of the amorphous structure remains elusive from both theoretical and experimental aspects. A spectrum of behavior from ferromagnetic metal to insulator is realized in one Co–Fe–Ta–B–O system via continuously compositional adjustability. Hence, the amorphous structure can be manipulated in a well controllable manner, leading to tunable optical, electrical and magnetic properties over a wide range. This will help to build a reliable relationship between the amorphous structure and properties of these amorphous materials.

(3) New design concepts and device structures should be proposed for this new type of AMSs, aiming to combine logic functionalities and information storage capabilities in a single device through manipulating the spin and charge simultaneously. This will facilitate the development of next-generation spintronic devices with low power, rapid response and high storage density.

Acknowledgments

We thank Prof. Cheng Song, Prof. Xiangrong Wang and Prof. Xiaozhong Zhang for profound discussions and comments. This work is sponsored by the National Key R&D Program of China (Grant No. 2017YFB0405704) and the National Natural Science Foundation of China (Grant No. 51471091).

References

[1] Holtzberg F, McGuire T R, Methfessel S, et al. Effect of electron concentration on magnetic exchange interactions in rare earth chalcogenides. Phys Rev Lett, 1964, 13, 18
[2] Kasuya T, Yanase A. Anomalous transport phenomena in Eu-chalcogenide alloys. Rev Mod Phys, 1968, 40, 684
[3] Methfessel S. Potential applications of magnetic rare earth compounds. IEEE Trans Mag, 1965, 1, 144
[4] Furdyna J K, Kossut J. Diluted magnetic semicondcutors. Vol. 25. In: Semiconductor and semimetals. New York: Academic Press, 1988
[5] Dietl T, Ohno H. Dilute ferromagnetic semiconductors: physics and spintronic structures. Rev Mod Phys, 2014, 86, 187
[6] Ohno H. Making nonmagnetic semiconductors ferromagnetic. Science, 1998, 281, 951
[7] Ohno H, Shen A, Matsukura F, et al. (Ga,Mn)As: A new diluted magnetic semiconductor based on GaAs. Appl Phys Lett, 1996, 69, 363
[8] Munekata H, Ohno H, von Molnár S, et al. Diluted magnetic III–V semiconductors. Phys Rev Lett, 1989, 63, 1849
[9] Chen L, Yang X, Yang F H, et al. Enhancing the Curie temperature of ferromagnetic semiconductor (Ga,Mn)As to 200 K via nanostructure engineering. Nano Lett, 2011, 11, 2584
[10] Matsumoto Y, Murakami M, Shono T, et al. Room-temperature ferromagnetism in transparent transition metal-doped titanium dioxide. Science, 2001, 291, 854
[11] Pulizzi F, Chambers S. Is it really intrinsic ferromagnetism. Nat Mater, 2010, 9, 956
[12] Chen L, Yan S, Xu P F, et al. Low-temperature magnetotransport behaviors of heavily Mn-doped (Ga,Mn)As films with high ferromagnetic transition temperature. Appl Phys Lett, 2009, 95, 182505
[13] Pulizzi F, Samarth N. A model ferromagnetic semiconductor. Nat Mater, 2010, 9, 955
[14] Ohno H. A window on the future of spintronics. Nat Mater, 2010, 9, 952
[15] Wang X L, Wang H L, Pan D, et al. Robust manipulation of magnetism in dilute magnetic semiconductor (Ga,Mn)As by organic molecules. Adv Mater, 2015, 27, 8043
[16] Editorial. More than just room temperature. Nat Mater, 2010, 9, 951
[17] Nie S H, Chin Y Y, Liu W Q, et al. Ferromagnetic interfacial interaction and the proximity effect in a Co_2FeAl/(Ga,Mn)As bilayer. Phys Rev Lett, 2013, 111, 027203
[18] Dietl T. A ten-year perspective on dilute magnetic semiconductors and oxides. Nat Mater, 2010, 9, 965
[19] Yu X Z, Wang H L, Pan D, et al. All zinc-blende GaAs/(Ga,Mn)As core-shell nanowires with ferromagnetic ordering. Nano Lett, 2013, 13, 1572
[20] Zhao J H. Is it possible to create magnetic semiconductors that work at room temperature. Chin Sci Bull, 2016, 61, 1401
[21] Hume-Rothery W. Phase stability in metals and alloys. New York: McGraw-Hill Book Company, 1966
[22] Hoistad L M, Lee S. The Hume-Rothery electron concentration rules and second moment scaling. J Am Chem Soc, 1991, 113, 8216
[23] Hume-Rothery W. The structure of metals and alloys. The Institute of Metals, London, 1939
[24] Chen N, Zhang Y Q, Yao K F. Transparent magnetic semiconductors from ferromagnetic amorphous alloys. Acta Phys Sin, 2017, 66, 176113
[25] Chen N, Li H P, Hirata A, et al. Transparent magnetic semiconductor with embedded metallic glass nano-granules. Mater Design, 2017, 132, 208
[26] Liu W J, Zhang H X, Shi J A, et al. A room-temperature magnetic semiconductor from a ferromagnetic metallic glass. Nat Commun, 2016, 7, 13497
[27] Inoue A. Stabilization of metallic supercooled liquid and bulk amorphous alloys. Acta Mater, 2000, 48, 279
[28] Johnson W L. Bulk glass-forming metallic alloys: science and technology. MRS Bull, 1999, 24, 42
[29] Greer A L. Metallic glasses. Science, 1995, 267, 1947
[30] Wang W H, Dong C, Shek C H. Bulk metallic glasses. Mater Sci Eng R, 2004, 44, 45
[31] Chen M W. A brief overview of bulk metallic glasses. NPG Asia Mater, 2011, 3, 82
[32] Coey J M D, Venkatesan M, Fitzgerald C B. Donor impurity band exchange in dilute ferromagnetic oxides. Nat Mater, 2005, 4, 173
[33] Inoue A, Shen B L, Koshiba H, et al. Ultra-high strength above 5000 MPa and soft magnetic properties of Co–Fe–Ta–B bulk glassy alloys. Acta Mater, 2004, 52, 1631
[34] Inoue A, Shen B L, Koshiba H, et al. Cobalt-based bulk glassy alloy with ultrahigh strength and soft magnetic properties. Nat Mater, 2003, 2, 661
[35] Sharma P, Kimura H, Inoue A. Observation of unusual magnetic behavior: spin reorientation transition in thick Co–Fe–Ta–B glassy films. J Appl Phys, 2006, 100, 083902
[36] Sharma P, Kimura H, Inoue A, et al. Temperature and thickness driven spin-reorientation transition in amorphous Co–Fe–Ta–B thin films. Phys Rev B, 2006, 73, 052401
[37] Lucas M S, Bourne W C, Sheets A O, et al. Nanocrystalline Hf and Ta containing FeCo based alloys for high frequency applications. Mater Sci Eng B, 2011, 176, 1079
[38] Pellegren J P, Sokalski V M. Thickness and interface-dependent crystallization of CoFeB alloy thin films. IEEE Trans Magn, 2015, 51, 3400903
[39] Bader S D, Parkin S S P. Spintronics. Ann Rev Condens Matter Phys, 2010, 1, 71

[40] Ohno H, Chiba D, Matsukura F, et al. Electric-field control of ferromagnetism. Nature, 2000, 408, 944
[41] Song C, Cui B, Li F, et al. Recent progress in voltage control of magnetism: materials, mechanisms, and performance. Prog Mater Sci, 2017, 87, 33
[42] Žutić I, Fabian J, Das Sarma S. Spintronics: fundamentals and applications. Rev Mod Phys, 2004, 76, 323
[43] Hellman F, Hoffmann A, Tserkovnyak Y, et al. Interface-induced phenomena in magnetism. Rev Mod Phys, 2017, 89, 025006
[44] Awschalom D D, Flatté M E. Challenges for semiconductor spintronics. Nat Phys, 2007, 3, 153
[45] Weisheit M, Fähler S, Marty A, et al. Electric field-induced modification of magnetism in thin-film ferromagnets. Science, 2007, 315, 349
[46] Cui B, Song C, Mao H J, et al. Manipulation of electric field effect by orbital switch. Adv Funct Mater, 2016, 26, 753
[47] Cui B, Song C, Wang G Y, et al. Reversible ferromagnetic phase transition in electrode-gated manganites. Adv Funct Mater, 2014, 24, 7233
[48] Yamada Y, Ueno K, Fukumura T, et al. Electrically induced ferromagnetism at room temperature in cobalt-doped titanium dioxide. Science, 2011, 332, 1065
[49] Zhang Y Q, Zhao S F, Song C, et al. Electric-field control of ferromagnetism in a Co–Fe–Ta–B amorphous alloy. Mater Design, 2018, 143, 65
[50] Zhang S, Zhao Y G, Xiao X, et al. Giant electrical modulation of magnetization in $Co_{40}Fe_{40}B_{20}$/ $Pb(Mg_{1/3}Nb_{2/3})_{0.7}Ti_{0.3}O_3$ (011) heterostructure. Sci Rep, 2014, 4, 3727
[51] Liu Y T, Agnus G, Ono S, et al. Ionic-liquid gating of perpendicularly magnetised CoFeB/MgO thin films. J Appl Phys, 2016, 120, 023901
[52] Nakano M, Shibuya K, Okuyama D, et al. Collective bulk carrier delocalization driven by electrostatic surface charge accumulation. Nature, 2012, 487, 459
[53] Narushima S, Mizoguchi H, Shimizu K, et al. A p-type amorphous oxide semiconductor and room temperature fabrication of amorphous oxide p–n heterojunction diodes. Adv Mater, 2003, 15, 1409